BBAA VI International Colloquium on:
Bluff Bodies Aerodynamics & Applications
Milano, Italy, July, 20-24 2008

PRESSURE DISTRIBUTIONS AND FLOW FIELDS IMPOSING EXTREME WIND FORCE COMPONENTS

Yukio Tamura[*], Hirotoshi Kikuchi[†], Nadaraja Pillai[#], and Kazuki Hibi[†]

[*]Wind Engineering Research Center
Tokyo Polytechnic University, 1583 Iiyama, Atsugi shi, Kanagawa 243-0297, Japan
e-mails: yukio@arch.t-kougei.ac.jp, snada@vestas.com

[†]RIT, Shimizu Corporation, Etchujima 3-4-17, Koto-ku, Tokyo, Japan
e-mails: h_kikuchi@shimz.co.jp, hibi@shimz.co.jp

[#]Vestas Technology R&D Chennai Private Limited
MRC Nagar, R.A.Puram, Chennai – 600028, India
e-mail : snada@vestas.com

Keywords: Pressure distribution, Wind force combination, Absolute value correlation, Maximum wind force, Flow field, PIV

INTRODUCTION

Huge numbers of samples were analyzed for low-rise building models and ensemble averaged instantaneous pressure patterns causing extreme wind forces are shown in Tamura et al. [1]. It's also reported in Tamura et al. [2] that instantaneous wind pressure distributions are never symmetric even when along-wind force reaches a maximum. Therefore, in order to reflect actual maximum load effects in structural design of buildings, combination of these wind force components should be considered. It is commonly known that along-wind force fluctuations are mainly generated by approaching flow turbulence, but the dominant cause of crosswind force and torsional moment fluctuations is vortex shedding. Thus, it had been believed that crosswind force and torsional moment were well correlated, but along-wind force was not correlated with the other two components. Tamura et al. [3] explained that in design of low- and medium-rise buildings, along-wind response was generally predominant, but that their combinations tended to be ignored. Along-wind and crosswind combinations for tall buildings and structures have been discussed by Melbourne [4], Vickery & Basu [5] and Solari & Pagnini [6]. This paper discusses the results in terms of phase-plane expression, cross correlation, absolute value correlation, simultaneously occurring wind force components when the other is maximum and so on for the building models. Flow patterns around building models causing some extreme conditions in the surface pressure field are also discussed.

INSTANTANEOUS WIND PRESSURE DISTRIBUTIONS CAUSING MAXIMUM WIND FORCE COMPONENTS

All the instantaneous extreme pressure distributions, i.e. the 154 samples, were superimposed and the typical extreme pressure distributions causing the maximum wind force components were

extracted and are shown in Fig.1. As the pressure distributions can cluster to the right or left side from sample to sample, if they were superimposed as they were, a pressure distribution similar to the mean pressure might be obtained rather than the typical pressure distribution. Therefore, the above superimposition, or conditional averaging was made after turning the right and left of some data to orientate the direction of the torsional moment or crosswind force. The ensemble averaged extreme pressure distributions causing the maximum along-wind force coefficient C_{Dmax} and torsional moment coefficient C_{Tmax} have a similar asymmetric pressure pattern, as shown in Figs.1(a) and 1(c).

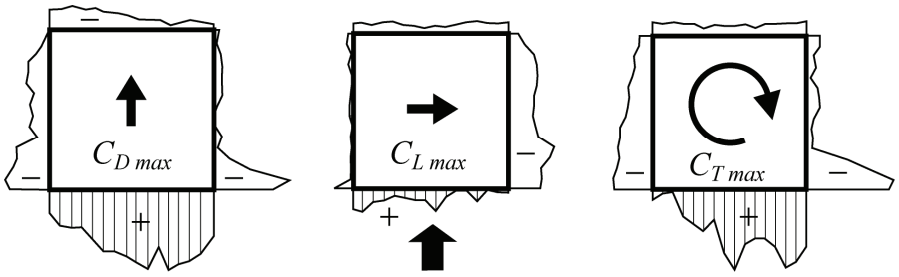

(a) Causing C_{Dmax} (b) Causing C_{Lmax} (c) Causing C_{Tmax}

Figure 1: Examples of instantaneous pressure distributions causing maximum wind force coefficients for model LS (α = 1/4) [3]

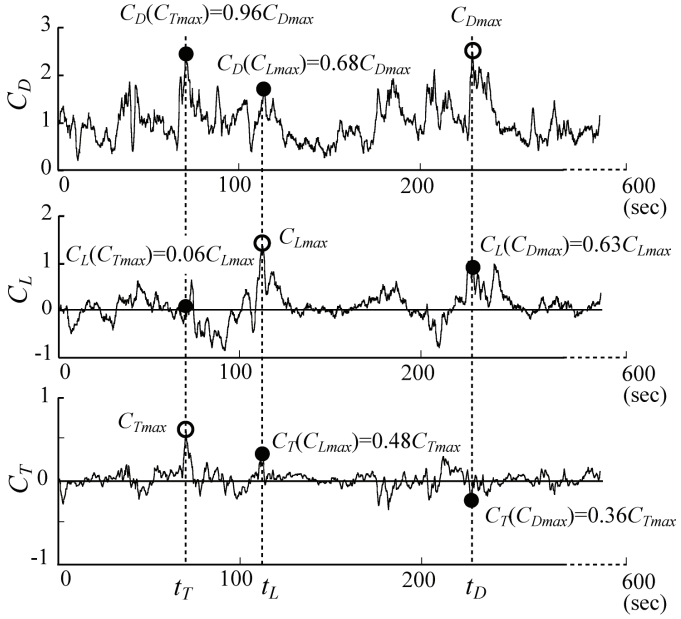

Figure 2: Maximum wind force component and accompanying other wind force components (LS) [3]

MAXIMUM WIND FORCE COMPONENT AND OTHER SIMULTANEOUSLY OBSERVED WIND FORCE COMPONENTS

Figure 2 shows an example of temporal variations of three wind force components of a 10-min sample in full-scale conversion. The maximum value of one of the wind forces, i.e. C_D, C_L or C_T, was selected and the other two simultaneously recorded wind forces were picked up. When the maximum along-wind force C_{Dmax} was recorded at time t_D, some large $C_L(C_{Dmax})$ was also

recorded. When the maximum torsional moment C_{Tmax} was recorded at time t_T, well-correlated crosswind force $C_L(C_{Tmax})$ became relatively small, but un-correlated along-wind force $C_D(C_{Tmax})$ reached almost its largest level.

CORRELATION AND ABSOLUTE VALUE CORRELATION BETWEEN WIND FORCE COMPONENTS

A very low correlation is recognized between C_D - C_L, and also between C_D - C_T. The former coincides with the aforementioned results, demonstrating a low correlation between the maximum values of along-wind force coefficient C_D and crosswind force coefficient C_L. However, the latter does not coincide with those results, suggesting a high correlation between the maximum values of torsional moment coefficient C_T and along-wind force coefficient C_D. However, some correlation is recognized between C_L - C_T, although their maximum values do not correlate. These contradictory relations between the average correlation of the time series and the correlation of the maximum values can be partly understood by examining the cross-correlation coefficient between the absolute values of wind force components as follows. For the absolute values of the wind force components, the largest correlation was recognized between the along-wind force coefficient $|C_D|$ and the torsional moment coefficient $|C_T|$. This is consistent with the fact that the maximum torsional moment tends to be accompanied by the largest level of along-wind force. The lowest correlation was recognized between the crosswind force coefficient $|C_L|$ and the torsional moment coefficient $|C_T|$.

FLOW FIELDS AND PIV MEASUREMENTS

The phase-plane expression for $C_D - C_L$ shown in Fig.3 for the low-rise square model (LS) shows an elliptical shape and indicates no correlation between the along-wind and crosswind forces. An example of the instantaneous wind pressure distribution for which the maximum or minimum along-wind force occurs is shown in Fig.4. Figure 4(a) shows the instantaneous wind pressure distributions causing the maximum level along-wind forces indicated by open circles in Fig.3. Figure 4(a) shows an uneven distribution of large positive wind pressure on the windward wall. Figure 4(b) shows the instantaneous wind pressure distributions causing the minimum level along-wind forces indicated by open squares in Fig.3. The magnitudes of the positive pressure on the windward wall and the negative pressure on the side walls and the leeward wall are relatively small, and the resultant along-wind, crosswind and torsional components are all small. Ensemble averaged flow fields causing maximum and minimum along-wind forces are shown in Fig.5 for 20 samples. The length of each sample was 10min in full-scale conversion. Figure 5(a) shows the instantaneous pressure distribution and the flow field causing the maximum along-wind force.

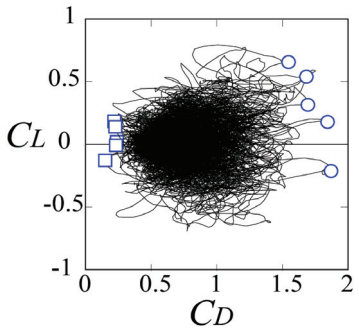

Figure 3: Phase-plane expression of wind force combination (C_D-C_L)

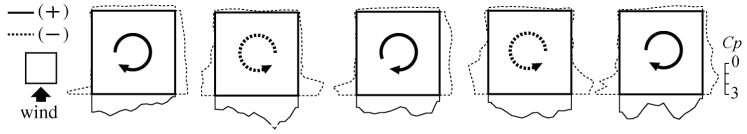

(a) causing maximum along-wind force C_{Dmax}

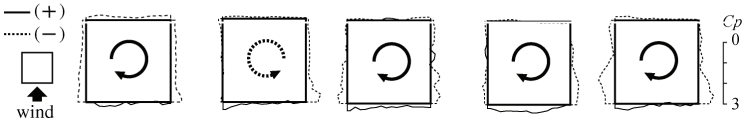

(b) causing minimum along-wind force C_{Dmin}

Figure 4: Instantaneous wind pressure distributions causing maximum /minimum wind force components (5*H*/8)

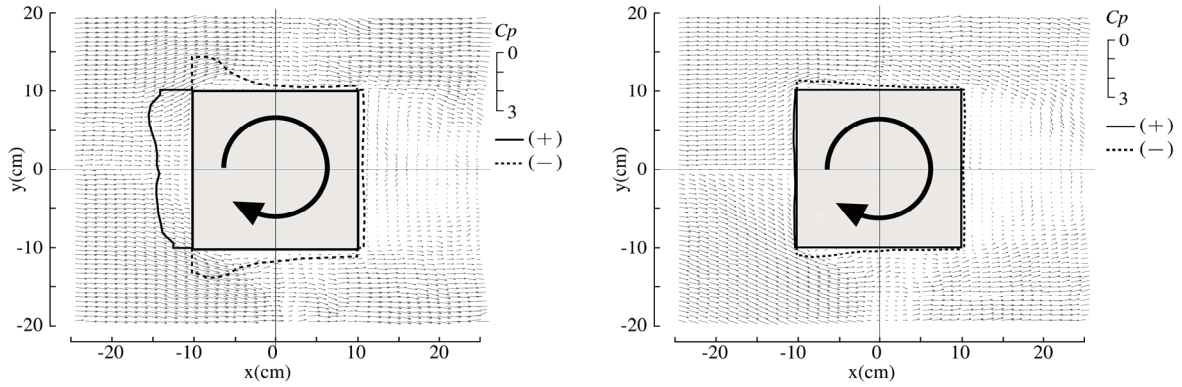

(a) causing maximum along-wind force C_{Dmax} (b) causing minimum along-wind force C_{Dmin}

Figure 5: Ensemble-averaged instantaneous wind pressure distributions and flow fields causing maximum/minimum along-wind force components (5*H*/8)

A separation bubble and re-attachment are observed near the leading edge and the trailing edge of the upper side, respectively, in Fig.5(a). Figure 5(b) shows the case for the minimum along-wind force. An almost symmetrical pressure distribution with very small magnitude is observed, thus providing the smallest level of along-wind, cross-wind and torsional components. Very small pressures on the windward and leeward walls are especially noteworthy.

CONCLUDING REMARKS

This paper has summarized the findings of an extensive research carried out on wind pressure distributions causing extreme wind force components by the authors' group for various types of building models. Phase-plane expressions between wind force components were examined and the variations of their loci with the wind direction were also discussed. The importance of the cross-correlation coefficients of the absolute values of wind force components for examining wind force combinations was demonstrated. The maximum wind force component and simultaneously observed other wind force components were also examined and discussed. Finally, some representative flow patterns causing extreme wind force components were discussed on the basis of DPIV measurements of flow fields.

REFERENCES

[1] Y. Tamura, H. Kikuchi, K. Hibi, Extreme wind pressure distributions on low-rise building models, *Journal of Wind Engineering and Industrial Aerodynamics*, **89**, 1635-1646, 2001.
[2] Y. Tamura, H. Kikuchi, K. Hibi, Wind load combinations and extreme pressure distributions on low- rise buildings, *Wind and Structures*, *An International Journal*, **3** (4), 279- 289, 2000.
[3] Y. Tamura, H. Kikuchi, K. Hibi, Quasi-static wind load combinations for low- and middle-rise buildings, *Journal of Wind Engineering and Industrial Aerodynamics*, **91**, 1613-1625, 2003.
[4] W.H. Melbourne, Probability distributions of responses of BHP house to wind action and model comparison, *Journal of Wind Engineering and Industrial Aerodynamics*, **1** (2), 167-175, 1975.
[5] B.J. Vickery, R.I. Basu, The response of reinforced concrete chimneys to vortex shedding, *Engineering Structures*, **6**, 324- 333, 1984.
[6] G. Solari, L.C. Pagnini, Gust buffeting and aeroelastic behavior of poles and monotubular towers, *Journal of Fluids and Structures*, **13**, 877-905, 1999.